

A Review on the Impact of Icing on Aircraft Stability and Control.

(Received: June 18, 2009. Revised: Aug. 08, 2010. Accepted: Sept. 13, 2010)

WOUTIJN J. BAARS¹
RONALD O. STEARMAN²
CHARLES E. TINNEY³

Abstract

Several years of earlier research was conducted for the U.S. Air Force, related to the impact that warhead-induced damage had on the aeroelastic integrity of lifting surfaces and in turn the resulting upset of the complete aircraft. This prompted us to look at how similar aeroelastic events and aircraft upsets might be triggered by ice accumulation on specific parts of the aircraft. Although seldom studied, icing can also significantly impact the aircraft's aeroelastic stability, and hence the overall aircraft stability and control, and can finally result in irreversible upset events. In this latter context, classical flutter events of the lifting surfaces and controls can occur due to ice-induced mass unbalance or control hinge moments and force reversals. Also, a loss of control effectiveness caused by limit cycle oscillations of the controls and lifting surfaces may appear, due to significant time-dependent drag forces introduced by separated flow conditions caused by the ice accumulation. A review is presented in this article on the mechanisms that initiate these ice-induced upset events when considering the class of small general aviation aircraft. The review is based on literature and earlier experimental work performed at The University of Texas at Austin. Two commonly observed ice-induced aircraft stability and control upset scenarios were selected to investigate. The first upset scenario that is presented involves an elevator limit cycle oscillation and a resulting loss of elevator control effectiveness. The second upset is related to a violent wing rock or an unstable Dutch Roll event.

1. Introduction

Ice accumulation on aircraft, and the resulting aerodynamic unsteadiness and possible stability upsets of the entire aircraft, are undesired. Research on these upsets is of high importance, since ice protection systems are not able to completely eliminate the presence of ice accumulation on aircraft. Structural ice formation on leading edges of wings and control surfaces initiate significant regions of unsteady flow [1]. This change in the performance of the lifting surfaces can result in a major change in handling of the aircraft; the aircraft may stall at higher speeds, the stall angle of attack may decrease and irreversible upset events can be initiated.

In the period of 1990 - 2000, a total of 3,230 aircraft accidents were recorded by the Air Safety Foundation. Twelve percent of those were related to icing [2]. In one type of aircraft, most of the icing accidents occurred during the approach and landing phases [3, 4, 5], when the aircraft was flying at a higher angle of attack when compared to cruise flight. Studies on ice-related accidents of small general aviation aircraft have revealed that in many cases even the most experienced pilots have less than 5 to 8 minutes to escape the harmful icing conditions before their aircraft experiences violent upsets. This suggests that in cruise the accumulation of ice, and its effect on the stability of the aircraft, remain mostly unobserved. Upon changing the attitude of the aircraft, the formation of ice induces unsteady flow phenomena capable of upsetting the aircraft in a catastrophic manner.

¹ PhD Graduate Student, baars@mail.utexas.edu

² Professor, rstearman@austin.rr.com

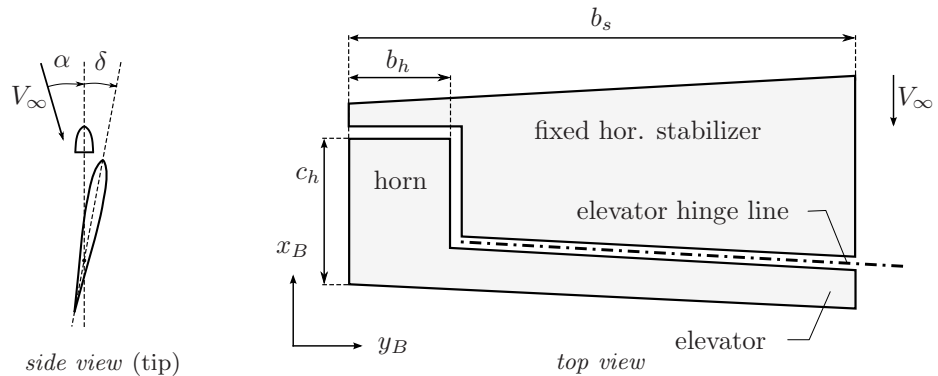
³ Assistant Professor, cetinney@mail.utexas.edu

Dept. of Aerospace Engineering & Engineering Mechanics, The University of Texas at Austin
210 E. 24th Street, W. R. Woolrich Laboratories, Austin, TX 78712, U.S.A.

Figure 1: Indication of the elevator horn balances on the aircraft and the orientation of the body-axis reference frame (x_B, y_B, z_B) and the aircraft's angle of attack α_a .¹



Figure 2: (top view) Schematic of LHS horizontal stabilizer and the location of the elevator and horn balance, (side view) the angle of attack α of the horizontal stabilizer and the elevator deflection angle δ .



A particular element of small general aviation aircraft that can act as a destabilizing source mechanism is the *elevator horn balance*. The elevator horn balances are located at the tip of the horizontal stabilizers as indicated in figures 1, 2 and 3. The elevator horn balance acts as an aerodynamic/mass balance that lowers the pilots control force needed to deflect the elevator and alleviates low flutter speeds associated with control surfaces found in reversible control systems. The aerodynamic chord of the horn balance, c_h , is relatively long when compared to the control horn span, b_h ; that results in a significant overhang and exposure of the leading edge of the horn balance to the freestream flow when the elevator is slightly deflected. This is the case during, for example, a climb maneuver or flare just before touchdown, which are the phases of flight where most of the accidents occur [3, 4, 5].

While aircraft that are certified to fly in icing conditions are equipped with anti-icing (preventive) and de-icing (repressive) ice protection systems, it is still possible for ice-induced upsets to occur. Namely, those repressive systems do not completely eliminate the ice accretion and associated effects, but have only the effect of partially preventing the ice accumulation. The upsets can occur through the remaining ice on the wing and stabilizers after a few boot de-icing cycles, so-called residual icing, or through icing that builds up in between the de-icing cycles, so-called intercycle icing. Aggravating this issue is the fact that the elevator horn balance is rarely equipped with an ice protection system. In the de-icing philosophy of ice protection on horn balances, no inflatable de-icing boots are employed since their activation causes significant control hinge moment variations thus upsetting the aircraft trim conditions in cruise flight.

This research article is a review of the mechanisms that initiate ice-induced aircraft stability and control upsets of small general aviation aircraft. Multiple mechanisms can be responsible for recorded ice-related accidents which are indicated by a Weibull failure analysis. After reviewing two NTSB Safety Recommendations (2004,2006) [4, 5], Airworthiness Directives from the FAA [3],

¹picture: Cessna Aircraft Company (<http://www.cessna.com/caravan/grand-caravan/grand-caravan-gallery.html>, retrieved 6 February 2010).

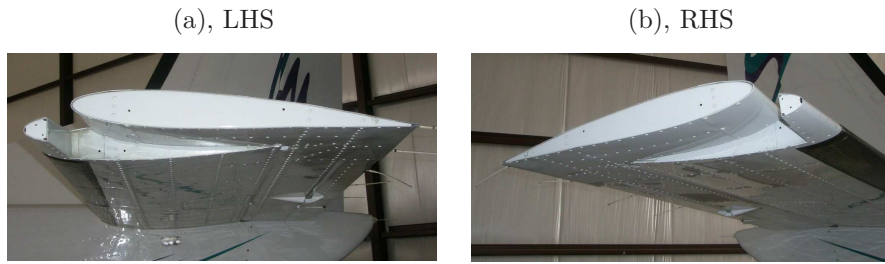


Figure 3: Elevator horn balances on a small general aviation aircraft.



Figure 4: Severe mixed ice accumulation on the tail of a full-scale NASA test aircraft [10].

and two pilot reports listed in the work of Endruhn *et al.* (2006) [6], two ice-induced destabilizing mechanisms of small general aviation aircraft have been identified. In this research article the plausible upset mechanisms are presented and related to earlier experimental and theoretical work that was performed at The University of Texas at Austin (UT Austin). The first destabilizing upset scenario, a loss of elevator control effectiveness, involves an elevator limit cycle oscillation (LCO) that is caused by an ice-induced unsteady flow field locking-in with the motion of the relative flexible elevator horn balance. This lock-in mechanism appears to be nonlinear in nature [7, 8, 9]. The second upset mechanism results in a violent wing rock or unstable Dutch roll event, caused by a coupling between the ice-induced separated flow field shedding frequencies ahead of the elevator horn balance and the fuselage cross flow shedding frequency. The latter upset will also be shown to be another nonlinear interaction between the Dutch roll frequency and unsteady flow frequencies induced by tail plane icing and elevator horn shielding.

2. Ice Accumulation on the Horizontal Tail

When the aircraft is flying through icing conditions, ice accumulates on all frontal exposed surfaces of the aircraft. On the leading edges of the wings and stabilizers, a commonly found ice horn protrudes normal to the surface. Such an ice formation on a tail leading edge of a full-scale NASA test aircraft is shown in figure 4.

Unique wind tunnel experiments were conducted at the NASA Glenn Research Center icing tunnel by Wilson (1967) [11] on a tail shielded horn balance (NACA 0006) in icing conditions. One of the experiments was performed at a free stream velocity of 90m/s and in sub zero temperatures (-10°C). The stabilizer was set at $\alpha = 0^\circ$ while the horn balance was deflected by $\delta = -4^\circ$. The mean volumetric diameter (MVD) and the liquid water content (LWC) were $15\mu\text{m}$ and 1.2gm/m^3 , respectively. These numbers represent typical icing conditions during cruise. The experiments showed significant accumulation of ice in the form of ice horns, on both the leading edge of the stabilizer and the lifting surface of the horn balance. Illustrations of the ice formation after a 5 and 7 minute exposure to these icing conditions are shown in figure 5. After 8 minutes, the horn balance started to show significant sub-critical-flutter events or LCOs. Wind tunnel studies performed by Tate & Stearman (1986) [9], using simulated icing, have demonstrated and validated this LCO behavior. It is interesting to note that the first known reporting of this control horn LCO occurred in September of 1917 by Fokker FR-1 pilots [8] while engaged in combat

Figure 5: Illustrations of the ice build-up on a stabilizer with shielded horn balance, extracted from the work of Wilson (1967) [11].

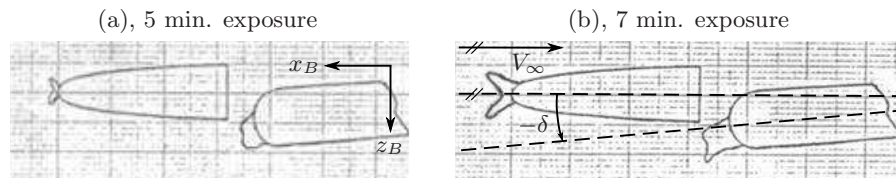
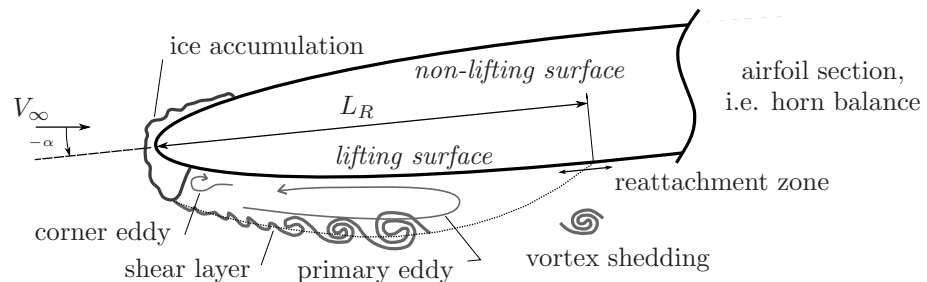


Figure 6: Schematic of the ice-induced separation bubble on an airfoil with leading edge ice accumulation, following the work of Gurbacki *et al.* (2004) [13].



operations during the first World War.

Several studies have been performed on the actual effects of (simulated) ice deposit on the leading edges of airfoils [12, 13, 14, 15]. A schematic indicating the typical flow features around an airfoil with leading edge ice formation is shown in figure 6. The air flow around the ice horn on the lifting surface of the airfoil separates due to an adverse pressure gradient. Downstream of the ice horn a primary eddy and corner eddy are present followed by a reattachment region and a vortex shedding event from the shear layer. The characteristics are consistent with the well-studied backward-facing step flows such as in review by Eaton & Johnston (1981) [16] and as presented in the study by Bradshaw & Wong (1972) [17].

The studies conducted by Gurbacki & Bragg (2002) [12] on a NACA 0012 airfoil ($Re_c = 1.8 \cdot 10^6$) with leading edge ice simulations showed an increase in mean reattachment length (the length of the separation bubble), L_R , with increasing angle of attack. At $\alpha = 0^\circ$ the reattachment point was located at $0.13c$, while at $\alpha = 8^\circ$ the separation bubble extended over the full chord of the airfoil [12]. Broeren *et al.* (2004) [14] indicated that the ice simulation causes a large increase in L_R at $\alpha = 6^\circ$. Furthermore, Bragg & Khodadoust (1992) [15] concluded, based on an experiment on a NACA 0012 airfoil ($Re_c = 1.5 \cdot 10^6$) with leading edge ice simulation, that it is likely that at $\alpha = 6^\circ$ the bubble is highly unstable. At $\alpha > 6^\circ$ the flow is unable to overcome the adverse pressure gradient, resulting in an intermittent reattachment of the flow or no reattachment at all. This results in a bubble bursting phenomenon that can initiate a premature airfoil stall across the entire span (the stall angle of attack for a clean NACA 0012 airfoil is $\alpha_{stall} = 16^\circ$ [18]). Busch *et al.* (2008) [19] concluded that the horn at the non-lifting surface is less critical, because small variations of this horn cause only a difference in the drag coefficient at low angles of attack. Since the experiments at UT Austin, cited in this article, were conducted with a non-flexible horn balance, only one simulated ice shape was attached to the lifting surface of the horn balance leading edge. It is to be noted that the ice horn at the non-lifting side is important in general due to its mass influence on the control surface and its effect on aeroelastic phenomena.

A qualitative wind tunnel visualization study was conducted at UT Austin [20] to validate the occurrence of unsteady flow events downstream of the ice accumulation. Figures 7 and 8 indicate the span wise vorticity structures and the flow separation over the horn balance for $\alpha = 0^\circ$ and $\delta = -8^\circ$. It was observed that the two dimensional span wise vorticity signatures were still present although highly three dimensional flow effects were observed at the stabilizer tip.

Unsteady flow features resulting from the ice-induced separation bubble were experimentally investigated by Gurbacki & Bragg (2004) [13] on a NACA

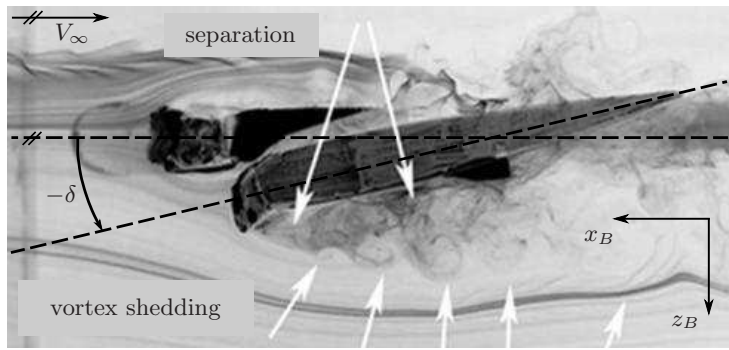


Figure 7: Flow visualization over a $1/10^{\text{th}}$ scale LHS horizontal stabilizer with elevator horn balance using a smoke wire sheet producing a 2d smoke sheet (*side view*), $\alpha = 0^\circ$, $\delta = -8^\circ$, $Re_{c_h} = 1.7 \cdot 10^5$ [20].

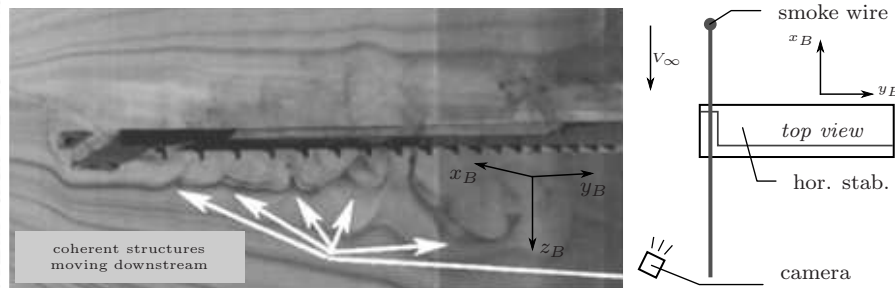


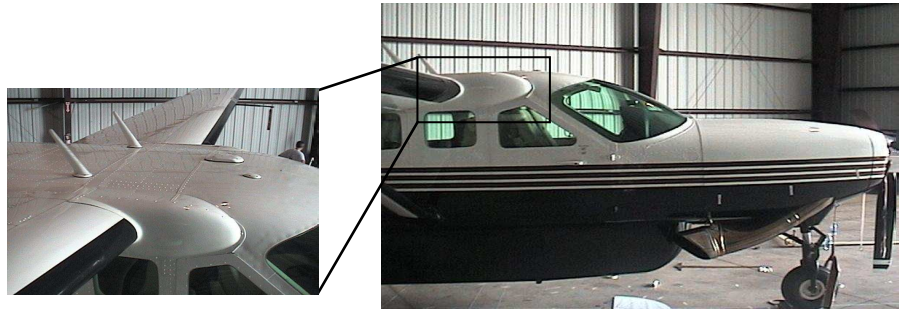
Figure 8: Flow visualization over a $1/10^{\text{th}}$ scale LHS horizontal stabilizer with elevator horn balance using a smoke wire sheet producing a 2d smoke sheet (*oblique view*), $\alpha = 0^\circ$, $\delta = -8^\circ$, $Re_{c_h} = 1.7 \cdot 10^5$ [20].

0012 airfoil. The first unsteady flow feature, quantified by a Strouhal number based on the free stream velocity V_∞ and the reattachment length L_R of $St_{L_R} = f \cdot L_R / V_\infty = 0.53$ to 0.73 [13], is associated with the shear layer vortex structures (vortex movement in and aft of the shear layer) and is referred to as the regular mode. This mode was found by spectral analysis of time-dependent surface pressure measurements at the chord wise position where the separation bubble reattached. Likewise, spectral analysis of lift and moment coefficients captured by a three component balance system revealed the second unsteady flow feature, corresponding to a Strouhal number of $St_{L_P} = f \cdot L_P / V_\infty = 0.0048$ to 0.0101 [13], where $L_P = c \cdot \sin(\alpha)$ is the projected airfoil height and c is the mean aerodynamic chord of the airfoil. This mode is referred to as the low-frequency mode and is often associated with shear layer flapping. In this study the linear and nonlinear coupling between the two unsteady measurements was not analyzed. The unsteady quasi-harmonic 'motion' of the structure can actually be a result of nonlinear lock-in of the structure with the unsteady quasi-harmonic, ice-induced, flow features as outlined by Baars *et al.* (2009) [21].

3. Relevant Aircraft Features during Upset Mechanisms

The small general aviation aircraft are Part 23 FAA Federal Aviation Regulation (FAR) certified aircraft that are mostly propeller driven vehicles with features somewhat different than those found on the larger Part 25 FAR aircraft that are more often turbine powered and much higher performance aircraft. With the increasing take-off and landing cycles each year, the small general aviation aircraft are statistically more exposed to potential icing conditions for a greater percentage of flight time than aircraft flying longer routes and at higher altitudes, such as the larger, Part 25 FAR, jet aircraft. Although Part 23 aircraft are certified to fly in icing through 14 CFR Part 23, this 14 CFR Part 23 refers to the 14 CFR Part 25 appendix for icing certification, so the icing requirements are equivalent. However, some differences are found between Part 23 and 25 aircraft. In a Part 23 aircraft, for example, the flight control systems are generally activated directly by pilot manual input and are reversible. The control systems are not of the hard hydraulic irreversible types that are typically found on fighter aircraft and larger Part 25 aircraft. The implication is that the

Figure 9: A 'shoulder' located at the wing/fuselage junction on the RHS of a small general aviation aircraft.



general aviation control surfaces can be activated by hand through a manual oscillation or movement of the control surfaces. This cannot be done on aircraft with irreversible controls. From the point of view of aircraft upset events, an aerodynamic input external to the pilot, such as an aerodynamic gust, can force the controls into an action that could overpower the pilot control input when the aircraft has reversible controls. This could upset the stability and control of the total aircraft.

Most of the reversible control surface systems employ a combined aerodynamic and mass balance horn, incorporated in an external control surface as was indicated in figures 2 and 3. This horn balance alleviates low flutter speeds associated with control surfaces found in reversible control systems. In the de-icing philosophy of ice protection on horn balances no inflatable de-icing boots are employed since their activation causes significant control hinge moment variations upsetting the aircraft trim conditions in cruise flight.

3.1 Fuselage Characteristics

3.1.1 Wing Root Leading Edge Shoulder

A wing root vortex is originated at the wing root leading edge/fuselage junction. This vortex is the result of the oncoming flow at the wing root that has the tendency to deflect to the top of the fuselage due to the relative low pressure zone here. Therefore, the two wing root vortices have the same orientation as the well-known wing tip vortices. In addition, for some small general aviation aircraft the strength of the wing root vortices is increased by the vortices trailing off from the so-called 'shoulders' at the wing root leading edge/fuselage junction as indicated in figures 9 and 12. It is believed that these 'shoulders' are there to generate extra vortical lift, because an elliptical shaped body, placed under a slight angle with respect to the oncoming flow, generates a vortex.

Water tunnel studies have been performed by Stearman *et al.* (2005) [22] on a representative $1/32^{nd}$ scale aircraft model to confirm the existence of the wing root vortex pair. Similar studies were performed in the low-speed wind tunnel facility of UT Austin where quantitative total pressure contours were acquired with a total head pressure rake [22]. The vortical regions show up as low pressure zones. At $\alpha_a = 0^\circ$ (α_a is the aircraft's angle of attack, see figure 1) the vortex pair would trail below the horizontal stabilizers, as indicated in figure 10a. When increasing the angle of attack to $\alpha_a = 6^\circ$, the vortex pair would trail at the same level as the location of the horizontal stabilizers, shown in figure 10b. For $\alpha_a = 10^\circ$ the vortex pair is clearly located above the horizontal stabilizers and next to the vertical tail as shown in figure 10c. Furthermore, it was observed that when the aircraft is in a conventional landing approach or climbing mode the vortex pair would be above the horizontal stabilizers and next to the vertical stabilizer as well [6].

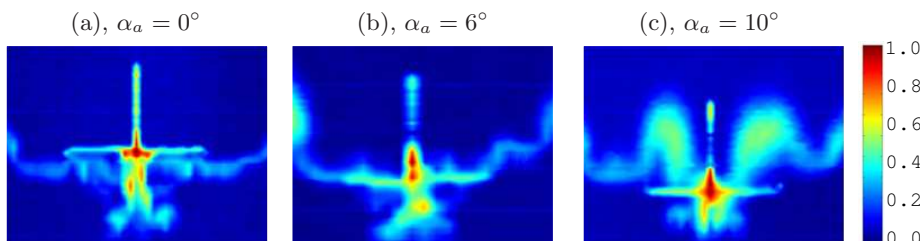


Figure 10: Contours of the total pressure ratio $1 - p/p_\infty$ behind a $1/32^{nd}$ scale model of a small general aviation aircraft, $Re_{\bar{c}_{wing}} = 85,000$ [22].

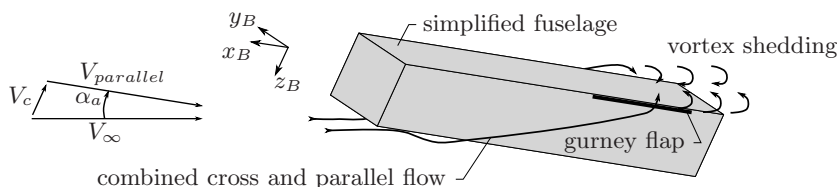


Figure 11: Schematic of the cross flow around a simplified fuselage at a positive angle of attack α_a (note that the longitudinal edges of the fuselage are rounded in reality).

3.1.2 Longitudinal Gurney Flaps

The last important characteristic concerning the discussion of the upset events are the drip plates mounted above the rear doors of the fuselage as indicated in figure 12. Those drip plates act as gurney flaps relative to the cross flow, to ensure that the separation points of the cross flow around the fuselage are fixed. The cross flow V_c occurs when the aircraft is flying at a positive angle of attack, $\alpha_a > 0^\circ$, as schematically indicated in figure 11. The trailing edge vortical unsteadiness originating from the wing root is further aggravated when the fuselage chines or drip plates, holding these root vortices to the fuselage, also ice up. The ice deposit blunts the sharp aerodynamic chines, which can then no longer hold these two wing root trailing vortices to the fuselage. This will produce two alternately moving separation points.

4. Proposed Ice-Induced Destabilizing Mechanisms

This section starts off with the identification of multiple destabilizing or failure mechanisms related to icing for a representative small general aviation aircraft. Two failure mechanisms are selected for study, which are introduced by pilot and witness reports. The failure mechanisms are discussed in detail in the last two sections 4.3 and 4.4.

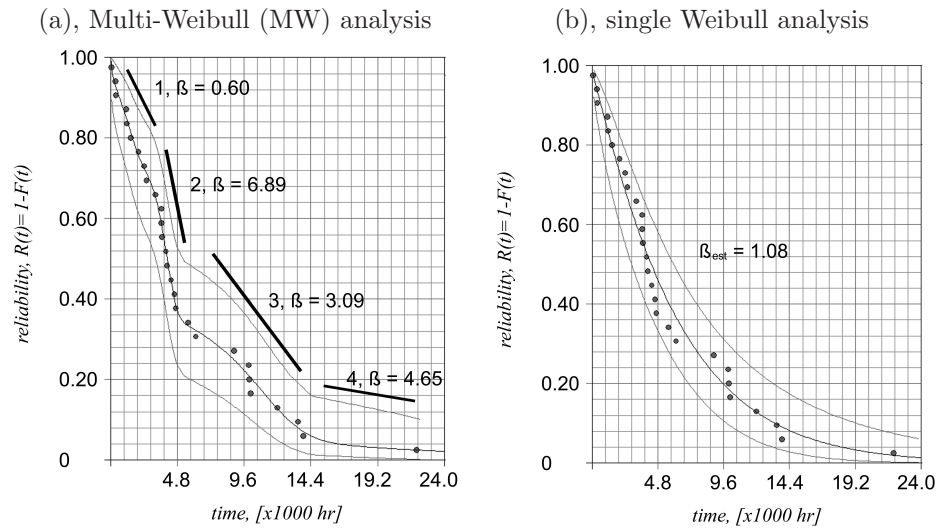
4.1 Weibull Failure Analysis

A Weibull failure analysis of published NTSB icing accident data, for a representative small general aviation aircraft, was accomplished by employing the Weibull commercially available software. This software has one of several analyses options known as the Multi-Weibull (MW) subroutine. This was developed for the case where the accident data input is known to have multi-failure modes



Figure 12: Indication of the 'shoulder', gurney flap and elevator horn balance on the LHS of a small general aviation aircraft.

Figure 13: Weibull failure analysis of the published NTSB icing accident data, figure (a) indicates the identification of four failure modes with its respective slopes β . Generated by ReliaSoft's Weibull++ 5.0 software.



embedded within it. The presence and approximate number of failure modes that appear within the input dataset can be estimated by first assuming the presence of only one failure mode in the input dataset and running a traditional single Weibull failure analysis. A careful review of the resulting Weibull reliability and unreliability output data plots will then illustrate different groupings of failure modes through the so-called "dog legs" in these plotted functions. That is, the data will group in what appears as different segmented straight lines defined by smaller numbers of output data points. Each grouping of data points can then be connected by jogs or "dog legs" in the output data plots. The number of such straight line segments is a first estimate of the number of failure modes. Even though the NTSB accident data has been prescreened to include only accidents occurring in the presence of atmospheric icing conditions in practice, several different failure modes in the dataset are still known to be present. These different upset or failure modes could involve ice-induced tail or wing stall or malfunction of different elements of the de-icing systems, for example.

The object of the MW analysis is to determine the Weibull fit lines from one general dataset involving mixed failure modes without requiring initial input data censoring or categorization into different data failure sets. The MW input data analysis option determines the Weibull fit lines from this one, generally mixed, dataset involving multiple failure events, which have all occurred while the aircraft is flying in icing. The resulting MW analysis output would, in essence, be different Weibull fit lines first identifying 'infant mortality' or 'early failures' as well as 'random failures' (Weibull line slope β less than or equal to 1.0) followed by 'wear out' (Weibull slope greater than 1.0). The general perspective of the reliabilities for each observed failure mode, are produced by individual straight lines, which when taken together give a resultant curved line on the overall Weibull graph simulating the entire range of product life as described by the well known bath-tub curve. This model of the failure rate or hazard rate of the human life cycle was first adopted by the insurance companies. It was later adopted to model the reliability of mechanical systems [23].

An estimate of the overall reliability of this representative general aviation aircraft, when flying in icing conditions, is shown when estimated by the MW approach in figure 13a, demonstrating an estimated four failure modes in the 28 point dataset. The slope β of the first and most critical Weibull line is 0.60 which is seen to lie well within the 'infant mortality' or 'early failures' region of the bath-tub curve. The other three failure modes lie outside the 'infant mortality' failure zone into the 'wear out' region. Finally, a typical Weibull failure analysis using a single line slope estimate, produces the reliability function illustrated in

figure 13b. The resulting "dog legs" in this reliability estimate of the 28 point dataset suggest at least four failure modes as well. The slope β of this single Weibull line approaches the random failure slope of 1.0. The estimated value is close to this, being $\beta_{est} = 1.08$, as shown in figure 13b. Since multi-failures are admitted, the single line analysis is suggesting that any of the multiple failures could occur randomly across any of the possible failure modes.

4.2 Pilot and Witness Reports of Two Failure Modes

Of the four possible failure modes suggested in the Weibull failure analysis, two were chosen for analysis that were also identified in pilot and witness reports to the FAA/NTSB. One of the failure modes is initially triggered with the aircraft in a normal cruise attitude with no apparent significant icing condition observed on the wings, lift strut, or windshield. The upset occurred by a sudden onset of a LCO of the elevator, creating a fluttering of the elevator control column. This LCO of the elevator stalled the aircraft and pitched it over into a dive. A complete elevator control ineffectiveness then occurred in the dive with no way for the pilot to recover. In a last desperate move the pilot activated the de-icing system which initiates the tail de-icing first. The removal of the horizontal tail ice re-established the elevator control effectiveness and averted a fatal accident. A brief description of this ice-induced upset is presented in the following pilot report.

Narrative, Upset Number I: (quotation, listed in ref. [6]) *Acft. was in light rime ice at 9,000ft M.S.L. The wings and windshield were showing light rime ice accumulation, but not enough to warrant turning the boots on. The pitot static and prop heat were already on. The aircraft yoke started to flutter and almost immediately the aircraft stalled and pitched over into a dive. The elevator would not respond to any pilot elevator input, but only to pilot rudder and aileron input. I turned the pneumatic boots on while in the dive and regained elevator ctl. at approximately 4,800ft M.S.L.. I regained level flight at approximately 4,000ft M.S.L.. I then proceeded to climb to 7,000ft M.S.L. where I remained for the rest of the flight at a temp. of +2 degs. C. The main reason I wanted to rept. this is that similar circumstances occurred to me approx. 14 months ago. It would appear that the tail is accumulating more ice or is unable to carry as much ice as the main wing.*

Another pilot working for the same air freight company that reported the above two upsets, had a similar upset making a total of three similar upset events reported by the same air freight carrier. In summary, this upset event is triggered by an elevator limit cycle initiation for an aircraft in normal cruise attitude, which had no significant icing encounters based upon what the pilot observed in the way of only light ice deposits on the wings and windshield. This limit cycle event pitched the aircraft over into a dive where all elevator control was lost. Recovery back to an effective elevator control was only achieved after the removal of ice on the horizontal tail, averting three fatal accidents in this situation. There were two major unknowns to the pilots that experienced this upset scenario. First, in November 1991 the FAA and NASA sponsored an International Tailplane Icing Workshop where it was established that the tailplane is generally a more efficient collector of ice than the wing because it generally has a smaller leading edge radius than the wing. There have been reports of ice accretion on the tailplane 3 to 6 times thicker than ice on the wing [24]. The tailplane icing was therefore more extensive than the pilots realized by monitoring only the wing and windshield. Secondly, a difficulty occurred because little is known about the effects of icing on vortex generators that are mounted on the horizontal stabilizers and the exact mechanism as to how icing can disable their function. This item will be clarified in the analysis of this first upset.

$$\beta'' - \delta (a - b\beta^2) \beta' + [\bar{k}_0 - 2\delta (a - b\beta^2)^2] \beta = 0, \quad (1)$$

where β is a non-dimensional angle ϕ , $a = (\varepsilon - 1)$, $b = \varepsilon\bar{\eta}/2l$, $\bar{\eta}$ a non-dimensional shear layer geometry, and δ & k_0 are non-dimensional parameters. For a complete derivation and description of the aeroelastic model the interested reader is referred to Tate & Stearman (1986) [9]. Usually, the drag force element will only be significant when icing is present. It will manifest its presence in an aerodynamic stiffness element that is most likely time-dependent in character. This brings in a possible Mathew-Hill character to the equations and a possibility for a quadratic nonlinearity to the already nonlinear form of the equations [7]. From figure 14 it is easy to rationalize why a LCO could be triggered for a sheltered control horn. That is, for the proposed model it is well-known that the equation of motion, Eq. (1), can exhibit relaxation oscillations (i.e. pulsing of the elevator horn, sometimes felt by the pilot in icing conditions) or a steady LCO occurring possibly at slightly higher velocities or for different icing parameters. This latter event is the case for the discussed category I upset event. For slender rectangular wings, the aerodynamic loads are impulsive in character and concentrated at the leading edge of the aerodynamic horn. By looking at figure 14, simple statics tells us that for slender body airloads, which act at the horn balance leading edge, the shear-layer-aerodynamics wants to suck the leading edge of the elevator horn out of the sheltering pocket of the stabilizer tip. Only sufficient elevator bending and torsional stiffness in the neighborhood of the horn geometry, friction in the control circuit, pilot input, and balancing or weather vaning opposing forces from the remaining elevator input can help prevent this from happening. Once the elevator horn pops out of the sheltering stabilizer pocket, the shear-layer-aerodynamic forces on the leading edge of the horn, based on slender body theory, will vanish once the leading edge is exposed to uniform flow. The elastic restoring forces move the horn back, producing a natural limiting amplitude and hence a LCO repeating oscillation.

To further understand the loss of elevator control issue, reference is made to a book on the Cessna Single Engine development story by William D. Thompson, Chief of Flight Test and Aerodynamics during the Caravan Development Days [26]. In one part of the book he comments on the Grand Caravan C208B development history which answers a question commonly asked by the layman and experts alike concerning why a row of vortex generators are added to the stabilizers just ahead of the elevator hinge line. The following is Thompsons answer to that question: *"A unique problem of marginal nose-down elevator power was observed in transitional out-of-trim flight evaluations. This was alleviated by a single row of vortex-generators on the top surface of the horizontal tail just ahead of the gap between the stabilizer and elevator."* Since most of these aircraft icing accidents occur in the landing glideslope approach and flaring maneuver, and little is known about the influence of icing on vortex generators, a study was initiated to investigate this issue. A lack of elevator nose down authority during a landing maneuver could give rise to an upsetting event during this critical transitional phase of flight.

Another study was initiated at UT Austin to obtain some insight on the influence of icing on vortex generator performance [27]. Very limited hints of hand written comments found in a flight test report for small general aviation aircraft, for example, indicated that the vortex generators located along the elevator hinge line did not seem to ice up to any degree of significance [28]. That is, the 3:1 to 6:1 tail-icing:wing-icing growth rate does not seem to hold in the limit of smaller radii lifting surfaces such as vortex generators. It seems that when there is vanishing frontal area for ice to deposit on, it will not build up. Then the question arises what mechanism is at work, if any, for ice to nullify the benefits of vortex generators? Results from an experimental wind tunnel study conducted at UT Austin [27] related to this question are shown

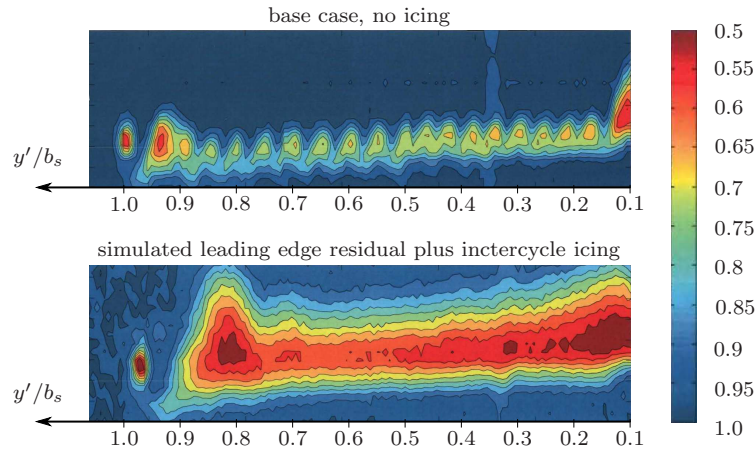


Figure 15: Contours of the total pressure ratio p/p_∞ behind a $1/10^{th}$ scale horizontal stabilizer [27], $\alpha = 6^\circ$, $\delta = 0^\circ$. $Re_{c_h} = 1.1 \cdot 10^5$.

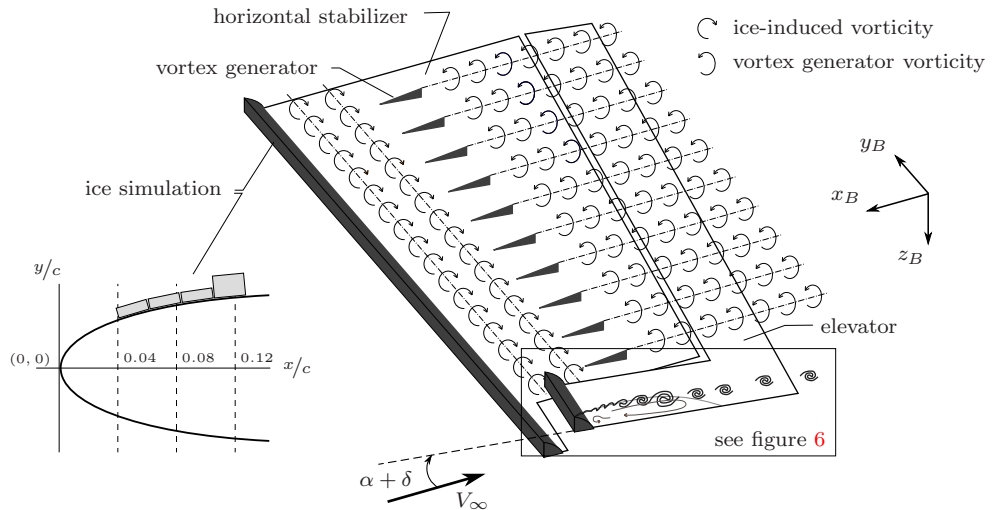


Figure 16: Schematic of the interaction between the ice-induced vortex field and the vortex field created by the vortex generators on a LHS horizontal stabilizer. The simulated ice accumulation that was used in the experiment at UT Austin is shown in the lower left corner [27].

in figure 15. A total head rake was run along the trailing edge of the stabilizer of our $1/10^{th}$ scale model with vortex generators to check the presence of the spanwise vorticity generated by the vortex generators. Figure 15 (top) illustrates a clean stabilizer where the generated vortices of each vortex generator is clearly seen in good detail. When simulated residual plus intercycle icing is applied to the stabilizer, as shown in the lower left corner of figure 16, a complete cancellation of the organized vorticity from the vortex generators is observed as shown in figure 15 (bottom). An examination of figure 16 suggests that an overlay of spanwise vorticity, shed off the ice-induced shear layer, is interacting with the orthogonally created vorticity by the vortex generators. In essence, the orthogonal overlay of these two distinct vorticity fields cancel each other. This action then nullifies the benefit of the vortex generators creating a loss of elevator pitch down control authority induced by icing conditions. In summary, if a LCO is also occurring, driven by the elevator iced up horns, as in the case of the category I upset, a much stronger spanwise bound vorticity is being shed which will certainly annihilate the benefit of the vortex generators. A complete loss of elevator control authority is then expected.

4.4 Upset No. II: Wing Rock

The category II "wing rock upset" in the present study was identified to be the first failure mode in figure 13a. The first point of 80 hours airframe time at upset and the point at airframe time of 3,227 hours at upset have specific been identified as observed violent aircraft upsets of the wing rock type. This upset described earlier under the pilot and witness reports has been observed in a number of accidents by several witnesses and has been experienced by at least

one surviving pilot [3, 4, 5, 6]. Seeking the opinion of an aerospace engineering expert on the subject, G. J. Hancock (1995) [29] states in his book that: "A key ingredient in wing rock is the loss of Dutch Roll damping". According to Hancock, wing rock can occur in at least three different forms which are itemized below:

1. Wing rock can occur in flow regimes where lag effects are not prominent; this form of wing rock is repeatable.
2. Wing rock can occur in flow regimes where lag effects due to onset of flow breakdown and reattachment, including vortex breakdown and reassembly, are prominent. This form of wing rock is sometimes random in occurrence with variations in amplitudes. Fore body vortices can play an influential role in this type of wing rock.
3. Persistent small amplitude irregular oscillations in roll can be generated at high subsonic speeds by asymmetric fore and aft movements of shock waves on the upper surface of the wing.

The first type of wing rock is most likely the one that is influencing the small general aviation aircrafts considered in this study, since their vortices are not developed from a fore body but the wing leading edge, implying that no prominent phase effects exist. This would allow a quasi-steady analysis with the dynamic terms and the airplane inertias in the equations of motion playing a less important role. It has also been observed in aircraft with well damped stability and control modes that the precise value of their three major inertias are not so critical to the study of their wing rock phenomenon.

The EA-6B Prowler, a twin-engine, electronic warfare aircraft, was exposed to stability and control upsets that were related to the pair of wing root vortices. Visualization studies were performed by Jordan, Hahne, Masiello & Gato (referenced by Bertin & Smith (1989) [30]) indicating that a pair of vortices was generated at the wing root leading edge. At low angles of attack those vortices were located below the horizontal stabilizers, as presented in figure 17a. At angles of attack below the stall angle the vortex pair trailed at the same location below the horizontal stabilizers due to the wing downwash. However, at angles of attack close to the stall angle, where the downwash effect of the wing was significantly reduced by the flow separation over the wing, the vortex pair was located above the horizontal stabilizers next to the vertical stabilizer as indicated in figure 17b. In case of a slight side slip, i.e. due to a gust, the vortex pair would flip over to one side of the vertical stabilizer, as indicated in figure 17c. The vertical stabilizer may now be exposed to a net force acting to the left hand side (low pressure zone in the vortex core). This has a direct impact on the directional stability of the aircraft by causing a yaw motion that can result in the stall of the right wing, because the aircraft's attitude was already close to the stall angle, causing a roll motion and thereby initiating the wing rock event. It is claimed that the EA-6B and the small general aviation aircraft having those wing root leading edge 'shoulders', have similar vortex interactions with the aircraft tail planes. This is claimed to be due to the fact that both wing root vortices originate from their wing root leading edges. In section 3.1 the pair of wing root leading edge vortices was introduced. Those wing root vortices are then shown to trail off from this wing root leading edge passing over the wing and ending up next to the vertical stabilizer as was shown in figure 10.

It was also concluded that a resulting violent wing rock motion occurred when the wing trailing vortex pair broke loose from the aerodynamic chines resulting in a fuselage cross flow vortex shedding motion, as was presented in figure 11. A study has been conducted at UT Austin on a $1/10^{th}$ scale, powered, radio-controlled, dynamic-cable-mounted, 6 DOF model, shown in figure 18. The observed fuselage cross flow shedding frequency of approximately

Figure 17: Directional destabilizing mechanism of the wing root vortex pair on the EA-6B [30].

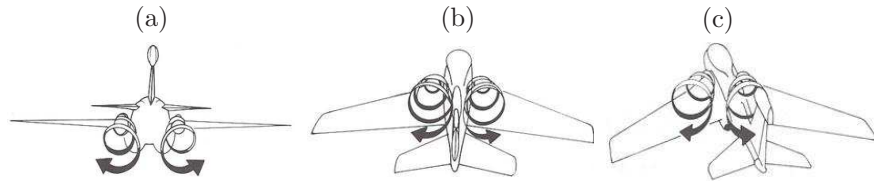


Figure 18: Cable-mounted model in the low-speed wind tunnel facility [27].



1Hz locked-in with the unsteady separated flow frequencies of 10Hz and 20Hz over the elevator horn balances, caused by the simulated ice accumulation, in a combination resonance mode. To deal with the nonlinear aspects of these vortex dynamic interactions, Higher Order Spectra (HOS) analysis techniques [31, 7] were used in the signal processing employed in the wind tunnel testing. Although the ice-induced unsteady flow phenomenon had different frequencies (measured using a pressure transducer near the elevator horn balance as 10Hz and 20Hz) and the Dutch Roll wing rock frequency (measured using accelerometers as 1Hz), it was concluded based upon cross-bicoherence analysis, that a lock-in of these three separate frequencies occurred in a quadratic sense, only when icing was present on the horn balance leading edges [6]. Figure 19 presents a plot of the cross-bicoherence function illustrating these events by demonstrating spectral peaks at coordinates of 10Hz and 1Hz as well as at 20Hz and 1Hz. It is evident from figure 19 that other interactions also appear possible.

Highspeed camera screenshots, presented in figure 20, indicate that the wing root vortices become very violent when the lock-in occurs, as they flip over to the other side. In this study by Endruhn *et al.* (2006) [6] it was also shown that if the aerodynamic chines or drip plates were extended back along the fuselage to about 0.5m (in full-scale size) forward of the leading edge of the horizontal stabilizers, the wing rock instability was suppressed. In essence, the highspeed video taping of this event also indicated that the extended chines actually hold the vortices down and away from the vertical stabilizer, so no cross flow can induce yawing and rolling of the aircraft as shown in figure 17c of the EA-6B aircraft.

Figure 19: Cross-bicoherence function of the pressure transducer and z-component of the accelerometer when ice was simulated on the elevator horn balance leading edges [6]. Ω_f and ω indicate the frequencies of respectively the acceleration and pressure events.

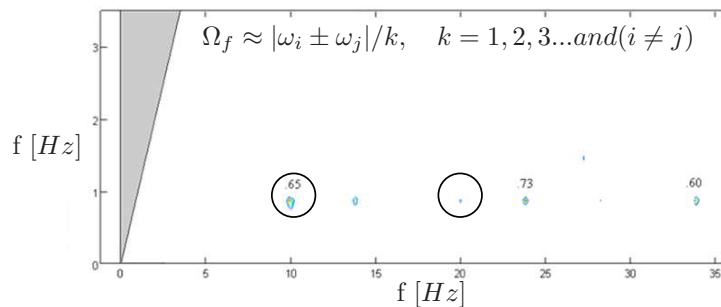




Figure 20: Highspeed camera screen shots showing the violent wing root vortices. The boxes highlight the tuft, attached to the farside of the fuselage, aft of the trailing edge, flipping over to the nearside.

5. Concluding Remarks

Two known general aviation aircraft icing upset scenarios were investigated to determine if some insight could be obtained as to the actual mechanisms causing the upsets. One upset involved an elevator horn ice-induced limit cycle oscillation of the elevator followed by a complete loss of elevator control authority. The second upset investigated involved an iced up elevator control horn inducing a violent wing rock or unstable Dutch Roll response. Both of these problems were investigated by employing wind tunnel testing and higher-order spectral signal processing as the primary investigative tools.

It was demonstrated that the loss of elevator control authority encountered in the first upset was due to a spanwise vorticity shedding off the shear layer of the separation bubble, caused by leading edge icing, which, wind tunnel tests show, will occur even in the absence of a limit cycle oscillation. This vorticity is approximately orthogonal to the vortex generator vorticity which is incorporated to overcome a loss of elevator nose down trim authority of relative long-fuselage aircraft. The orthogonal overlay of two vortex fields, of the appropriate relative strength and wave length, will destroy both vorticity fields. This was demonstrated experimentally in the wind tunnel. When the elevator is in a state of limit cycle oscillation the continual shedding of the bound vorticity of the surface will utterly destroy any vorticity produced by the row of vortex generators on that surface. The obvious solution to this problem is to employ an anti-icing system on the elevator horn as well as to any other aerodynamic horn balance. Some commercial aircraft are now successfully employing the TKS² technology on aerodynamic control horn balances.

Wind tunnel studies were employed to investigate the Dutch Roll induced instability, also triggered by an iced up elevator aerodynamic control horn balance. Two potential areas proved to show promise for alleviating this problem. First again, the anti-icing procedures are recommended for the control horn balances to avoid rapid ice build-ups on these surfaces that always seem to occur if no ice protection is employed here. Secondly, the aerodynamic chines, also employed as drip plates for passenger rain protection, should be anti-ice protected. Namely, the two wing root trailing edge vortices, which are employed to enhance the aircraft vortex lift through aerodynamic chines, will no longer be held by the chines when they are blunted by the icing process. In addition, wind tunnel studies indicated that when the chines, that are even ice free, are extended by about half a meter on full-scale aircraft, they will hold these trailing vortices and will not allow a wing rocking event.

²Tecalemit Killfrost Sheep-bridge-Stokes (TKS) is an advanced anti- and de-icing system that squeezes ethylene glycol-based fluid through laser drilled porous titanium panels attached over the airfoil leading edges.

Acknowledgments

The authors would gratefully acknowledge Dr. Edward J. Powers, from the department of Electrical & Computer Engineering (UT Austin), for his advice on the Higher-Order Spectra analysis. The authors would also like to thank Dr. David B. Goldstein, his students, and Claus W. Endruhn (former graduate student), from the Dept. of Aerospace Engineering and Engineering Mechanics (UT Austin), for their earlier experimental work. Furthermore, Delft University of Technology is acknowledged since the first author was an exchange visitor from its Aerospace Engineering department when this work was performed. Our appreciation is also expressed to Arthur Alan Wolk and The Wolk Law Firm for their past financial support in the form of a Research Gift to UT Austin to study critical icing problems concerning small general aviation aircraft.

References

- [1] M. B. Bragg, E. Whalen, and S. Lee. Characterizing the effect of ice on aircraft performance and control from flight data. In *40th Aerospace Sciences Meeting and Exhibit*, Reno, Nevada, January 2002. AIAA.
- [2] Aircraft icing. Safety advisor - weather no. 1, Air Safety Foundation (AOPA), April 2008. <http://www.aopa.org/asf/publications/sa11.pdf> (retrieved 10 February 2010).
- [3] FAA Airworthiness Directives: The Cessna Aircraft Company Models 208 and 208B Airplanes, Federal Register, vol. 70, no. 57, p. 15223-15227. Department of Transportation, March 2005.
- [4] Safety Recommendation, A-04-64 through -67, December 15, 2004. National Transportation Safety Board, Washington, D.C. 20594, December 2004.
- [5] Safety Recommendation, A-06-01 through -03, January 17, 2006. National Transportation Safety Board, Washington, D.C. 20594, January 2006.
- [6] C. W. Endruhn, R. O. Stearman, and D. B. Goldstein. Higher order statistical signal processing studies on the impact of icing on aircraft stability and control including aeroelastic effects. In *47th Structures, Structural Dynamics, and Materials Conference*, pages 184–196, Newport, Rhode Island, May 2006. AIAA.
- [7] H. Park, R. O. Stearman, T. Kim, and E. J. Powers. Wind-tunnel studies of damaged-wing-induced limit cycle oscillations. *Journal of Aircraft*, 45(5):1534–1545, September 2008.
- [8] M. S. Kruger, C. W. Endruhn, and R. O. Stearman. A new look at galloping. In *46th Structures, Structural Dynamics & Materials Conference*, Austin, Texas, April 2005. AIAA.
- [9] R. Tate and R. O. Stearman. The aeroelastic instability of an elevator balance horn in a shear layer wake flow. In *General Aircraft Meeting and Exposition*, Wichita, Kansas, April 1986. Society of Automotive Engineers. Paper 861827.
- [10] Tailplane Ice on Twin Otter Flight. Nasa Technical Reports Server, Accession ID: C-1992-02275, NASA Glenn Research Center, March 1992.
- [11] C. F. Wilson. Icing tests of a horizontal tail shielded horn balance on a light twin engine aircraft PA-31. Report no. 1502, Piper Aircraft Corporation, Lock Haven, Pennsylvania, December 1967.

- [12] H.M. Gurbacki and M. B. Bragg. Unsteady aerodynamics measurements on an iced airfoil. In *40th Aerospace Sciences Meeting and Exhibit*, Reno, Nevada, January 2002. AIAA.
- [13] H.M. Gurbacki and M. B. Bragg. Unsteady flow field about an iced airfoil. In *42nd Aerospace Sciences Meeting and Exhibit*, Reno, Nevada, January 2004. AIAA.
- [14] A. P. Broeren, H. E. Addy, and M. B. Bragg. Flowfield measurements about an airfoil with leading-edge ice shapes. In *42nd Aerospace Sciences Meeting and Exhibit*, Reno, Nevada, January 2004. AIAA.
- [15] M. B. Bragg and A. Khodadoust. Measurements in a leading-edge separation bubble due to simulated airfoil ice accretion. *AIAA Journal*, 30(6), June 1992.
- [16] J. K. Eaton and J. P. Johnston. A review of research on subsonic turbulent flow reattachment. *AIAA Journal*, 19(9), September 1981.
- [17] P. Bradshaw and F. Y. F. Wong. The reattachment and relaxation of a turbulent shear layer. *Journal of Fluid Mechanics*, 52(1):113–135, 1972.
- [18] I. H. Abbott and A. E. von Doenhoff. *Theory of Wing Sections - Including a summary of airfoil data*. Dover Publications Inc., New York, 1959.
- [19] G. T. Busch, A. P. Broeren, and M. B. Bragg. Aerodynamic simulation of a horn-ice accretion on a subscale model. *Journal of Aircraft*, 45(2), March 2008.
- [20] C. Newman and *et al.* Force Reactions from the Effects of Icing on a Caravan Stabilizer. Department of Aerospace Engineering and Engineering Mechanics, The University of Texas at Austin, 2004.
- [21] W. J. Baars, C. E. Tinney, and R. O. Stearman. Higher-order statistical analysis of stability upsets induced by elevator horn icing. In *27th Applied Aerodynamics Meeting and Exhibit*, San Antonio, Texas, June 2009. AIAA.
- [22] R. O. Stearman, D. B. Goldstein, and C. W. Endruhn. Progress Report on the Icing Studies of the Cessna 208B Grand Caravan. Center for Aeromechanics, Bureau of Engineering Research, The University of Texas at Austin, August 2005.
- [23] R. B. Abernethy. *The New Weibull Handbook, 4th edition*. Gulf Publishing Company, Houston, Texas, 2006. ISBN 0965306232.
- [24] Winter Operations Guidance for Air Carriers - And Other Adverse Weather Topics, CAC109225, 1992. Department of Transportation - Federal Aviation Administration, 1992.
- [25] A. Petre and H. Ashley. Drag effects on wing flutter. *Journal of Aircraft*, 13(10):755–763, October 1976.
- [26] W. D. Thompson. *Cessna - Wings for the World - The Single Engine Development Story, Second Printing*. Maverick Publishers, 1992.
- [27] J. Dearman and *et al.* The Effects of Icing on the Horizontal Stabilizer of a Cessna Caravan with Elevator Deflection. supervision D. B. Goldstein, Department of Aerospace Engineering and Engineering Mechanics, The University of Texas at Austin, 2007.
- [28] Delegation Option Manufacturer Flight Test Report - Flight into known icing conditions. Cessna Aircraft Company, Pawnee Division, Wichita, Kansas, September 1984.

- [29] G. J. Hancock. *An Introduction to the flight dynamics of rigid airplanes.* Imprint, New York, 1995.
- [30] J. J. Bertin and M. L. Smith. *Aerodynamics for Engineers.* Prentice Hall, Englewood Cliffs, New Jersey, 1989.
- [31] Y. C. Kim and E. J. Powers. Digital bispectral analysis and its applications to nonlinear wave interactions. *IEEE Transactions on Plasma Science*, 7(2):120–131, jun 1979.